Electronic Supplementary Material (ESI) for Dalton Transactions.

Properties of recombinant extracellular N-terminal domain of human high-affinity copper transporter 1 (hNdCTR1) and its interactions with Cu(II) and Ag(I) ions

Iurii A. Orlov, Tatiana P. Sankova, Alexey N. Skvortsov, Sergey A. Klotchenko, Elena I. Sakhenberg, Aleksandra A. Mekhova, Irina V. Kiseleva, Ekaterina Yu. Ilyechova,* Ludmila V. Puchkova

Electronic supplementary information

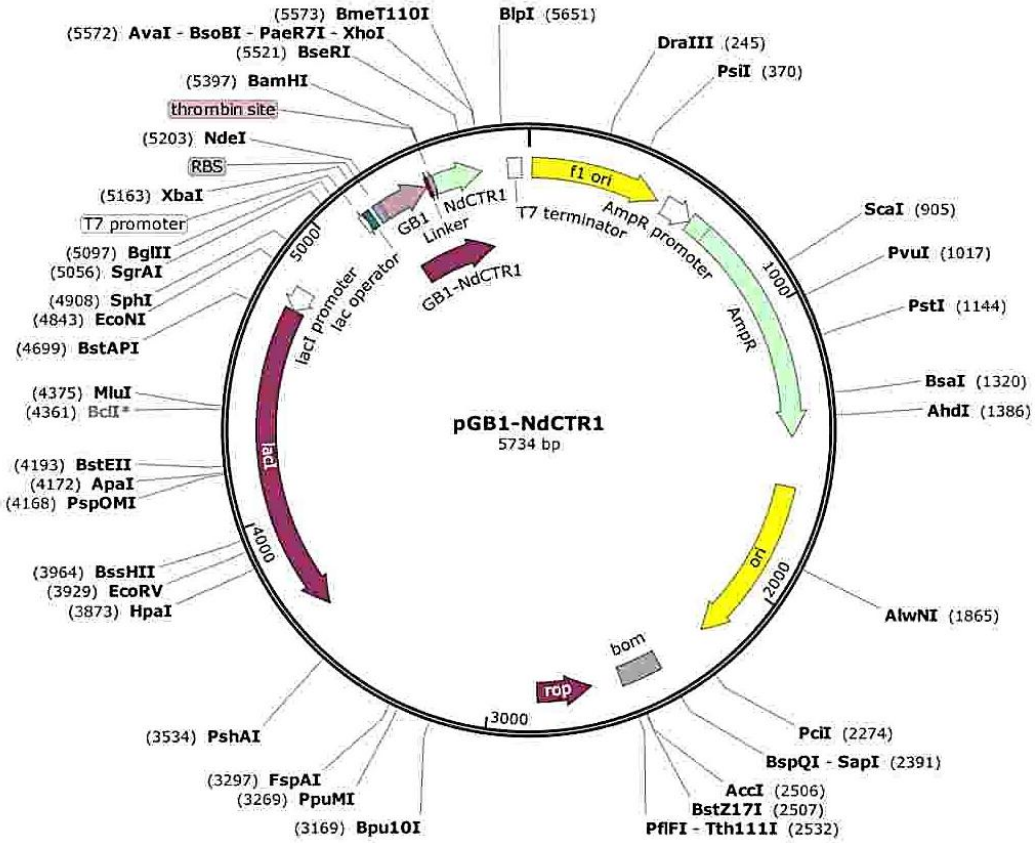

Fig. S1 Genetic map of pGB1–NdCTR1 plasmid.

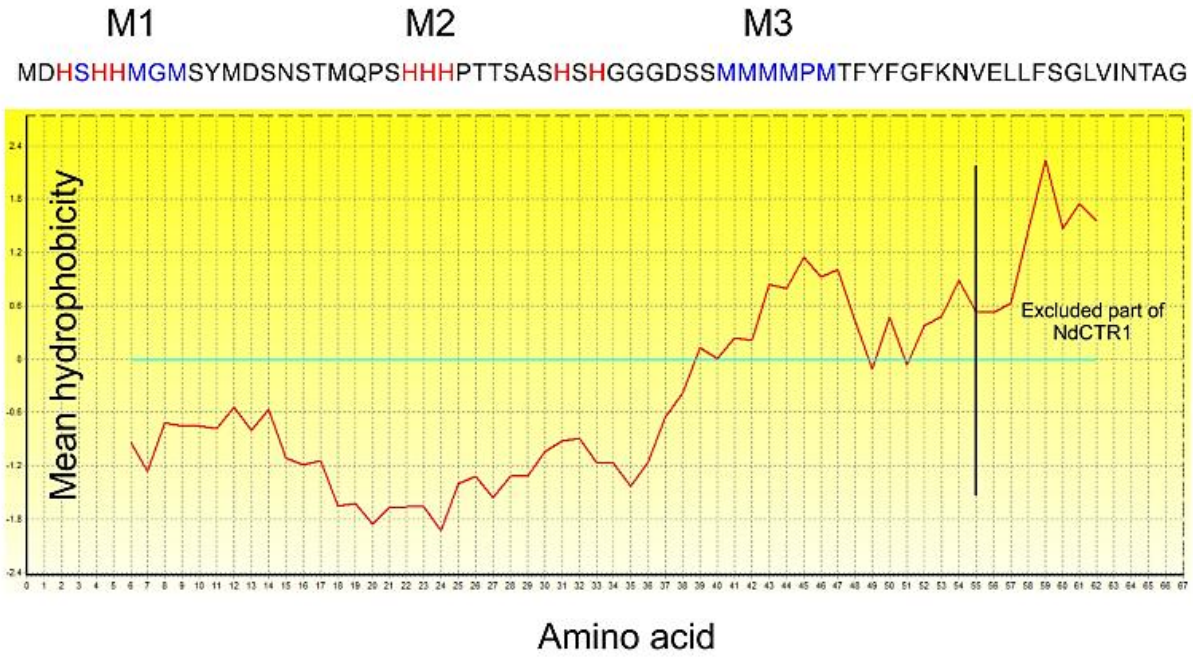

Fig. S2 Hydrophobicity profile of N-terminal 67-mer of human CTR1 protein.

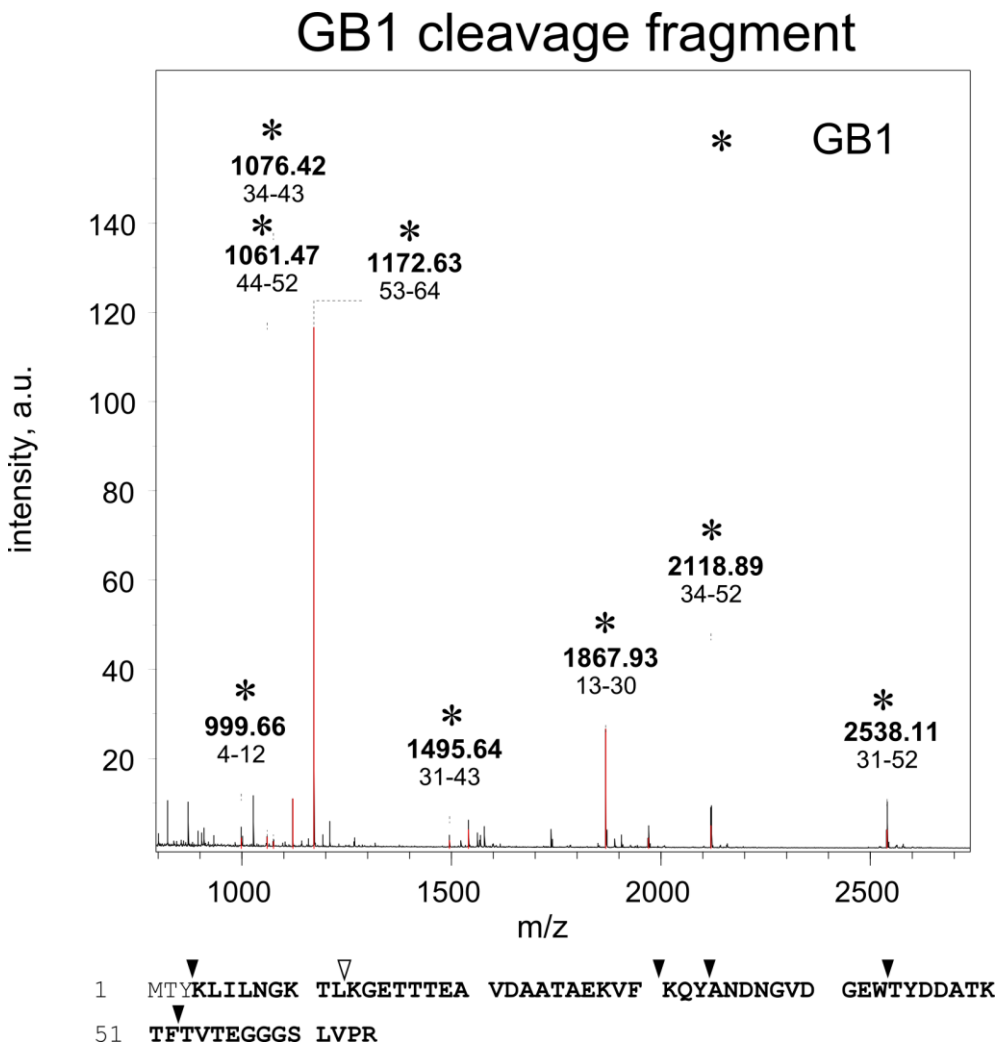

Fig. S3 MALDI mass spectrum of the protein band with the fastest mobility from the PAGE of the thrombin-treated GB1–NdCTR1, corresponding to GB1 fragment. The protein was treated by chymotrypsin. The m/z values and the aa ranges of the chymortypic fragments corresponding to GB1 are indicated. The sequence of GB1 with the position of cleavage sites and observed fragments are given below.

Table S1 List of primers and oligonucleotides used in standard PCR or synthesis of the sequences encoding NdCTR1 and the B1 domain of the immunoglobulin-binding protein G of streptococcus (GB1)

Name	T_m, ºC	Oligonucleotides sequence
NdCTR1-55_GB1_F	67.6	atcggatccatggatcattcccacc
NdCTR1-55_GB1_R	65.3	gtcctcgagattattccacattcttaaagc
GB1_bbF1	77.3	gtcacatatgacctataaactgatcctgaacggtaaaaccctgaaaggtgaaaccaccaccgaagctg
GB1_bbF2	79.2	ttcaaacagtatgcaaacgacaacggtgttgacggtgaatggacctatgacgacgcgaccaaaaccttt
GB1_bbR1	80.3	ccgttgtcgtttgcatactgtttgaaaacttttcggcggtggcggcgtcaacagcttcggtggtggtttcac
GB1_bbR2	81.3	tgcaggatccacgcggaaccagactacccccaccttcggtaacggtgaaggttttggtcgcgtcgtca

S4. Details of UV–Vis spectra analysis

The recorded spectra (200–1100 nm, N_0 1801) were corrected for cell/solvent absorption. It was assumed that the measured extinction D is a sum of characteristic absorption A (bands) and light scattering S. Light scattering was modeled by the conventional power model, $S = C_{scat}(\lambda/\lambda_0)^k$, where λ_0 is any constant reference point, which was selected at 200 nm, so that

$$D = A(\lambda) + C_{scat}(\lambda/\lambda_0)^k$$

For Rayleigh scattering, k equals minus 4, but the exact value is rarely observed, so k should be estimated by nonlinear fitting. In the studied systems, the true absorption of the system in the 320–500 nm range is the smallest, as it does not contain significant protein or copper bands there. Thus, fitting the scattering profile in this range is an estimate of the scattering item even if A is unknown. In the studied systems, all the components (proteins, solid AgCl particles, and Cu(II) complexes) show both absorption bands and scattering components. Scattering of pure protein solutions in buffer A is relatively low, with k ranging from -3 to -5; GB1–NdCTR1 protein displays relatively more scattering. Solid AgCl produces most Rayleigh scattering with k ~ –4 and band gap transition at ~240-250 nm (results match the findings in *Trinh D et al. Advances in Natural Sciences: Nanoscience and Nanotechnology. 2005. 6. 045011. doi: 10.1088/2043-6262/6/4/045011*), which partially overlaps with protein band. Cu(II):buffer A system has a rather complex spectral evolution, displaying a band in the 230–260 range, *d–d* bands in the red region with varying shape and scattering (apparently by Cu(II) hydroxides) at Cu(II) concentrations above 300 uM. As the protein band is overlapped with the bands of Cu(II)/Ag(I) species in the buffer and easily goes to the nonanalytic D>2.0 region, integral scattering of the system was selected as the major analytical figure.

The power model was fit using weighted symmetric least squares (LS) to the observed spectra in the 'non-absorbing' range:

$$R(C_{Scat}, k) = \Sigma_i w_i^2 (D(\lambda_i) - C_{scat}(\lambda_i/\lambda_0)^k)^2 \quad \lambda_i = [320..500] \text{ nm}$$

Logistic weights were selected to equalize the non-uniform noise of densitometric measurements (for details, see *Skvortsov A.N. // J. Chemom. 2017. doi: 10.1002/cem.2831*). Additionally, points with D>2.95 and points with an extreme second-order difference (spikes) were removed by assigning zero weights. C_{scat} for fixed k was estimated by linear LS, and k was optimized by Metropolis–Hastings stochastic search. The analytical figure presented in Figures 5 and 6 of the manuscript was a sum of scattering item $C_{scat}(\lambda_i/\lambda_0)^k$ over the 320-500 nm range; it is an indicator of nonresonant scattering of the system. Alternatively, the pure protein spectrum $A_{prot}(\lambda_i)$ was added to the model:

$$R(C_{prot}, C_{Scat}, k) = \Sigma_i w_i^2 [D(\lambda_i) - (C_{prot}A_{prot}(\lambda_i) + C_{scat}(\lambda_i/\lambda_0)^k)]^2 \quad \lambda_i = [260..500] \text{ nm}$$

The fitting was performed similarly but with two linear parameters for the fixed k. This model allowed us (a) to estimate absorption in the protein band and (b) to account for specific protein scattering in the system. In the proper scale of $A_{prot}(\lambda_i)$, C_{prot} is an apparent protein concentration, as estimated by its absorption, free from scattering bias. To reduce the noise, A_{prot} was constructed in the model by fitting cubic P-spline to measured protein spectra in buffer A (40 knots, smoothness penalty, validation with independently measured spectra). The second model did not produce reasonable results for strongly scattering spectra, as the 280 nm band was pushed out into the unobservable D>3.0 region. In such cases, C_{prot} was not assessed, and we used the first model.

Protein:Ag(I) systems were characterized mostly by plotting C_{scat} vs. total added [Ag(I)] and finding [Ag(I)] at which AgCl signal appeared (corresponding to the further inability of the system to bind Ag(I) stronger than chloride in $AgCl_s$, pK_d 9.75, pAg 8.9 in 0.15 M NaCl). The slope of this plot was not analyzed as AgCl scattering depends on particle quantity and particle size, which may be different in the presence of the protein. Protein:Cu(II) systems were analyzed for C_{prot} (if possible) and C_{scat}. In these systems, an increase in observed scattering over the small values of Cu(II):(buffer A) system indicated the formation of protein associates. This effect was observed only in GB1-NdCTR1:Cu(II) system but not in BSA:Cu(II) system. Titration of GB1-NdCTR1 with Cu(II) produced sigmoid dependence of scattering with an inflexion point at [Cu]/[protein] ~ 5; only part of the curve was observed for larger protein concentrations. Titration of Cu(II) stock with GB1-NdCTR1 produced peak dependence of C_{scat} on added protein, as expected from reversible protein association. The whole peak was observed at optimal [Cu(II)], but typically an upper or lower tail of the peak was observed. Notably, apparent protein absorption matched the expected absorption of the pure protein, indicating that the associates were well dispersed and did not precipitate. The varying *d–d* bands were observed in the>600 nm range, but they were not analyzed because of the potential bias from the used scattering model.